Biochemistry

 Volume 37, Number 24 June 16, 1998

Accelerated Publications

One-Third-the-Sites Transition-State Inhibitors for Purine Nucleoside Phosphorylase†

Robert W. Miles,‡ Peter C. Tyler,§ Richard H. Furneaux,§ Carey K. Bagdassarian,|| and Vern L. Schramm*,‡

Department of Biochemistry, Albert Einstein College of Medicine, Bronx, New York 10461, Carbohydrate Chemistry Team, Industrial Research Limited, Lower Hutt, New Zealand, and Department of Chemistry, The College of William and Mary, Williamsburg, VA 23187

Received March 20, 1998; Revised Manuscript Received April 29, 1998

ABSTRACT: Genetic defects in human purine nucleoside phosphorylase cause T-cell deficiency as the major phenotype. It has been proposed that efficient inhibitors of the enzyme might intervene in disorders of T-cell function. Compounds with features of the transition-state structure of purine nucleoside phosphorylase were synthesized and tested as inhibitors. The transition-state structure for purine nucleoside phosphorylase is characterized by (1) an elevated pK_a at N7 of the purine ring for protonation or favorable H-bond interaction with the enzyme and (2) oxocarbenium ion formation in the ribosyl ring (Kline, P. C., and Schramm, V. L. (1995) *Biochemistry 34*, 1153−1162). Both features have been incorporated into the stable transition-state analogues, (1*S*)-1-(9-deazahypoxanthin-9-yl)-1,4-dideoxy-1,4-imino-D-ribitol (immucillin-H) and (1*S*)-1-(9-deazaguanin-9-yl)-1,4-dideoxy-1,4-imino-D-ribitol (immucillin-G). Both inhibitors exhibit slow-onset tight-binding inhibition of calf spleen and human erythrocyte purine nucleoside phosphorylase. The inhibitors exhibit equilibrium dissociation constants (K_i*) from 23 to 72 pM and are the most powerful inhibitors reported for the enzyme. Complete inhibition of the homotrimeric enzyme occurs at one mole of inhibitor per mole of enzymic trimer. Binding of the transition-state inhibitor at one site per trimer prevents inhibitor binding at the remaining two sites of the homotrimer. A mechanism of sequential catalysis at each subunit, similar to that of F_1 ATPase, is supported by these results. Slow inhibitor dissociation (e.g., $t_{1/2}$ of 4.8 h) suggests that these compounds will have favorable pharmacologic properties. Interaction of transition-state inhibitors with purine nucleoside phosphorylase is different from reactant-state (substrate and product analogue) inhibitors of the enzyme which bind equally to all subunits of the homotrimer.

A genetic deficiency of T-cells results from mutations in the locus encoding for purine nucleoside phosphorylase (PNP) in humans (*1*). The mechanism for this exclusive tissue defect is related to the unique biology of T-cell function. Naive T-cells formed in the thymus each express one of a diverse repertoire of receptors for nonself epitopes. When antigen is presented to naive T-cells by the peptide•-MHC complex of B-lymphocytes, macrophages, or dendritic cells with appropriate costimulation, interleukin-2 is released and binds as an autocrine activator for rapid rounds of T-cell replication leading to a clonal expansion with activity against cells exhibiting the stimulatory antigen. However, most naive T-cells receive no antigenic signal and undergo apoptosis (*2*). Cellular nucleic acids from the apoptosed cells

†Supported by research Grant GM41916 from the National Institutes of Health.

* Corresponding author: Department of Biochemistry, Albert Einstein College of Medicine, 1300 Morris Park Avenue, Bronx, NY 10461. Tel: (718) 430-2813. Fax: (718) 430-8565. E-mail: vern@aecom.yu.edu.

‡ Albert Einstein College of Medicine.

§ Industrial Research Limited.

|| The College of William and Mary.

S0006-2960(98)00658-8 CCC: $15.00
Published on Web 05/28/1998

are recycled. The only enzyme which degrades deoxyguanosine in T-cells is purine nucleoside phosphorylase (PNP). Naive T-cells have the ability to transport and phosphorylate deoxyguanosine to dGTP, which accumulates relative to normal cells (*3*). T-Cell development in the thymus is inhibited by the presence of the deoxynucleotide imbalance by mechanisms which are not well defined. One proposal is that the allosteric inhibition of ribonucleotide reductase by dGTP for dUDP production (*4*) leads to an imbalance in the dNTP pool, preventing adequate DNA replication for T-cell maintenance. The levels of circulating T-cells fall to below 500/μL in human PNP deficiency (*1*). Inadequate clonal expansion of T-cells occurs in response to appropriate nonself signals, and the phenotype is T-cell immunodeficiency. Other hypotheses have been proposed, but recent deoxynucleotide metabolite data in PNP-deficient mice support the inhibition of ribonucleotide diphosphate reductase by dGTP (*5*, *6*).

Inappropriate activation of T-cells has been proposed or documented in several clinically relevant human conditions. They include transplant tissue rejection, psoriasis, rheumatoid arthritis, T-cell lymphomas, and autoimmune states including lupus. Inhibitor development for mammalian PNP has the intention of modulating the T-cell immune response in these conditions. Inhibitor design based on the X-ray crystal structure has provided a large number of inhibitors with dissociation constants in the nanomolar range (*7*−*9*). However, PNP is abundant in human erythrocytes, and tight-binding inhibitors in the picomolar range are more suitable to provide efficient inhibition of the enzyme in vivo. Our goal was to use the transition-state structure of PNP, determined from kinetic isotope effect studies, to design transition-state inhibitors.

The hypothesis for transition-state inhibitors is based on the proposal that the transition state is bound to the enzyme tighter than the substrate by a factor equal to the catalytic rate acceleration imposed by the enzyme. For PNP, this relationship predicts that an ideal transition-state inhibitor will bind with a dissociation constant of approximately 3×10^{-18} M (Figure 1). A transition-state structure for PNP from calf spleen was proposed recently on the basis of kinetic isotope effects (*10*). The results established that the enzyme stabilized a ribooxocarbenium ion and protonated N7 of the purine base to establish the transition state. X-ray crystallography with product and substrate analogue inhibitors indicates that Asn243 forms a H-bond to N7. The Asn243 interaction has been proposed to provide the electron-withdrawing role (*11*). The phosphate ion is not strongly involved in bond formation at the transition state, and thus the features of the transition state are localized in the nucleoside. In the absence of phosphate, the enzyme catalyzes the slow hydrolysis of inosine to form hypoxanthine and ribose with release of the ribose but noncovalent tight binding of the hypoxanthine (1.3 pM; *12*). The slow dissociation of tightly bound hypoxanthine permits isolation and characterization of the PNP•hypoxanthine complex, which contains one hypoxanthine per homotrimer, a consequence of one-third-the-sites catalytic reactivity. The unusual stoichiometry and the tight binding suggested that hypoxanthine is trapped by transition-state forces without the accompanying release of ribose 1-phosphate. This mechanistic feature is not unique to PNP, since the F_1 ATPase uses a reaction mechanism with

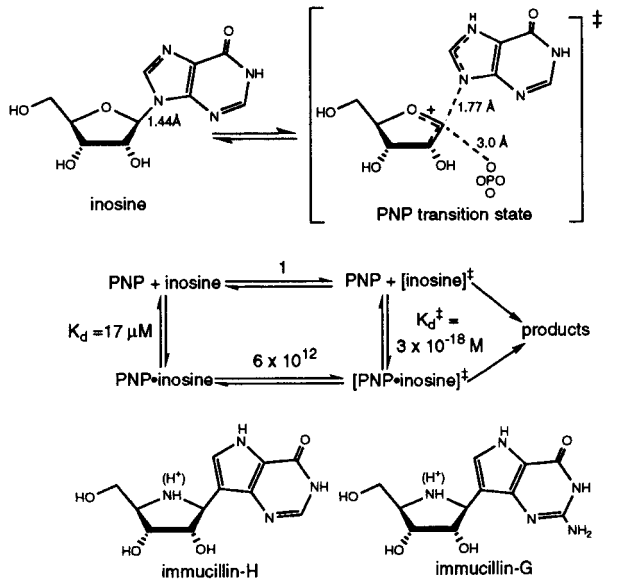

FIGURE 1: The structure of the transition-state for the reaction catalyzed by purine nucleoside phosphorylase (PNP) as deduced from kinetic isotope effects for the arsenolysis of inosine (upper panel; *34*, *35*). Binding energy of inosine at the transition-state is estimated from the rates of inosine hydrolysis at 30 °C, pH 7, relative to the catalytic efficiency of the enzyme in the presence of saturating inosine and phosphate (middle panel). The relative rates for the chemical and enzymatic reactions are from the hydrolysis of inosine by nucleoside hydrolase (*28*). The rate of uncatalyzed phosphorolysis is assumed from the known hydrolytic rate, since a rate for the chemical phosphorolysis of inosine is not available. Structures of the transition-state inhibitors for purine nucleoside phosphorylase: immucillin-H and immucillin-G are shown with protonation of the iminoribitol group (lower panel).

similar stoichiometry and tight binding of intermediates (*13*).

The physiological substrates for mammalian purine nucleoside phosphorylases are inosine, guanosine, and deoxyguanosine, with no significant activity against adenosine (*10*). The features of both guanine and hypoxanthine are incorporated into the inhibitors, but with elevated pK_a values at the N7 position accomplished by the use of 9-deazapurines. The charge or H-bond potential of the ribooxocarbenium ion is provided by the iminoribitol moiety with a stable ribosidic bond (Figure 1). These transition-state analogues are slow-onset, slow-release, tight-binding inhibitors for mammalian purine nucleoside phosphorylase. The picomolar dissociation constants and one-third-the-sites reactivity make these the most powerful inhibitors yet reported for PNP.

MATERIALS AND METHODS

Enzymes and Assays. Human (erythrocyte, lyophilized) and bovine (spleen, in 3.2 M ammonium sulfate) PNPs were purchased from Sigma and were the highest grades available. Human PNP powder was dissolved in 0.1 M sodium phosphate, pH 7.4, aliquoted in small glass tubes, rapidly frozen, and stored at −80 °C. Each sample was used only once after thawing. Enzyme from bovine spleen was diluted directly from the ammonium sulfate solution or after desalting. Enzyme preparations were estimated to be 85−90% pure on the basis of denaturing polyacrylamide gel electrophoresis. Some preparations of Sigma bovine PNP contained equal portions of apparent monomer (32 kDa) and dimers (64 kDa) of PNP on SDS gels. The specific catalytic activities and kinetics of inhibition were not influenced by

this apparent subunit heterogeneity. Enzyme concentration was determined from the extinction coefficient of 0.96 cm^{-1} at A_{280} for a 0.1% solution (*14*). The specific catalytic activity was 23−33 μmol min^{-1} mg^{-1}. Catalytic activity was determined in 50 mM potassium phosphate, pH 7.7, with variable inosine in the range from 40 μM to 5 mM. In a coupled assay, the hypoxanthine was converted to uric acid by including 60 milliunits of xanthine oxidase (buttermilk, Sigma Corp.) in the reaction mixtures, and by following uric acid formation at 293 nm which gave 12.9 mM^{-1} cm^{-1} (*15*).

Inhibitors. Inhibitors were synthesized by an extension of published methods (*16*) and will be reported elsewhere. Inhibitor concentrations were determined by the ultraviolet absorbance spectrum, using the published millimolar extinction coefficients of 9.54 at 261 nm and 8.92 at 269 nm at pH 7 for 9-deazainosine and 9-deazaguanosine, respectively (*17*).

Slow-Onset Inhibition. The slow onset of inhibition was measured by the addition of enzyme to complete assay mixtures at high substrate concentration (0.5−0.7 mM) and various inhibitor concentrations. Enzyme (0.4−6 nM final concentration) was added to assay mixtures followed by monitoring of product formation. Conditions for K_i* determination used high substrate concentration so that $I_t \gg E_t$ (*18*). Control experiments contained no inhibitor. K_i and K_i* were estimated by fitting initial and final steady-state rates against free inhibitor concentrations and using the equations for competitive inhibition under the conditions described by Morrison and Walsh (*18*). The rapidly reversible inhibition of PNP was analyzed by fitting to the following expression: $v_o = (k_{cat}A)/(K_m(1 + I/K_i) + A)$, where v_o is the initial reaction rate, A is substrate concentration, and I is the free inhibitor concentration. K_i* was analyzed by fitting to $v_s = (k_{cat}A)/(K_m(1 + I/K_i^*) + A)$, where v_s is the steady-state inhibited rate following attainment of equilibrium for the slow-onset step.

Inhibitor Release Studies. The enzyme and inhibitors were preincubated at the indicated concentrations for 3−4 h in 50 mM potassium phosphate, pH 7.7. At the indicated times, samples were diluted by factors of 1:10 000 to 1:1 000 000 into assay mixtures, and the rate of product formation was determined as a function of time. Control incubations included all components except inhibitor. To accommodate the slow rates for enzyme·inhibitor dissociation, high substrate concentrations (5 mM) and low enzyme concentrations were used.

Stoichiometry of Inhibitor Binding. Inhibitors were incubated with PNP for 3−4 h at room temperature in 50 mM potassium phosphate, pH 7.7. Samples were applied to Centricon ultrafiltration centrifuge tubes, and the unbound inhibitor was separated from the PNP·inhibitor complex. The filtrate was analyzed for inhibitor concentration by titration with PNP solutions of known concentration. Control experiments demonstrated that the ultrafiltration membrane did not retain inhibitors.

Similarity between Substrate, Inhibitors, and Transition State. The similarities of substrate and inhibitor to the transition state were determined with a similarity measure sensitive both to the electrostatic potential distribution on the molecular surfaces and to the surface geometries (*19*, *20*). The electron density and molecular electrostatic potentials of the molecules are calculated from ab initio techniques using *Gaussian 94* (*21*). The molecular three-dimensional geometries used for input are derived from gas-phase minimizations of *syn*-ribosyl starting configurations, with constraints on the transition-state bond angles and lengths that are derived from kinetic isotope effect measurements. The assumption is made that interactions with the enzyme cause all bound molecules to adopt similar configurations, and therefore, similar geometries are used. The molecules are superimposed for maximal coincidence. The Cube function of Gaussian 94 is used to calculate the electrostatic potential and electron density at all points in space for each molecule. The results of the similarity calculations have been found to be insensitive to the basis set (*20*). The chemical descriptor for similarity comparison is the molecular electrostatic potential at the van der Waals surface. For each molecule, this surface is created by extracting points that have electron density of approximately 0.002 electrons/$bohr^3$ from the Gaussian 94 output. Typically, a satisfactory surface is described with 50 surface points per atom. The Cartesian coordinates and electrostatic potential of each surface point are recorded. The similarity measure $\langle S_e \rangle$ is given by

$$\langle S_e \rangle = \frac{\sum_{i=1}^{nA}\sum_{j=1}^{nB} \epsilon_i^{A}\epsilon_j^{B} \exp(-\alpha r_{ij}^{2})}{\sqrt{\sum_{i=1}^{nA}\sum_{j=1}^{nA} \epsilon_i^{A}\epsilon_j^{A} \exp(-\alpha r_{ij}^{2})}\sqrt{\sum_{i=1}^{nB}\sum_{j=1}^{nB} \epsilon_i^{B}\epsilon_j^{B} \exp(-\alpha r_{ij}^{2})}} \quad (1)$$

where ϵ_i^B is the electrostatic potential at surface point i of molecule A, ϵ_j^B characterizes point j of molecule B, and in the numerator r_{ij}^2 is the distance squared between points i on A and j on B (eq 1). The double summation represents all interactions between the points of molecule A with the points on molecule B, and the similarity measure is thus a global comparison of electrostatic and geometrical similarity between the two molecules. The value α is the length scale for the interaction between two points, and the average similarity $<S_e>$ is calculated using three values $\alpha = 0.1$, 0.3, and 0.5 $Å^{-2}$. The denominator is used for normalization. If two molecules are identical to each other, $S_e = 1.0$, and this value decreases continuously as two molecules become increasingly less similar (*20*).

RESULTS AND DISCUSSION

Slow-Onset Inhibition and Inhibition Constants. The reaction rates of PNP in assays containing immucillin-H or immucillin-G exhibit modest inhibition in the initial reaction rate, with increasing inhibition as a function of time (Figure 2). The results are consistent with a two-step mechanism in which the inhibitor binds to form a reversible complex followed by a slow conformational change leading to a more tightly bound enzyme·inhibitor complex. The rate constant for onset of inhibition can be estimated from the expression $k = k_6 + k_5[(I/K_i)/(1 + (A/K_m) + (I/K_i))]$, where the terms correspond to the steps shown in eq 2 (*18*).

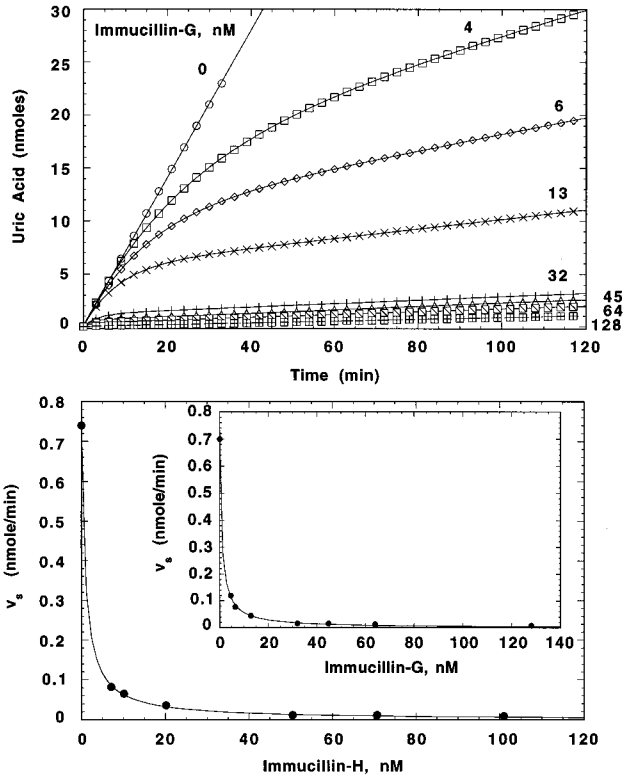

FIGURE 2: Slow-onset binding of bovine spleen PNP by immucillin-G (upper panel). The reaction was initiated by the addition of enzyme to reaction mixtures containing 700 μM inosine and the indicated concentrations of inhibitor. The enzyme concentration was 0.6 nM, and the reaction was monitored by coupling the formation of hypoxanthine to xanthine oxidase. The ordinate scale (nmoles of uric acid) is directly related to the 700 μM inosine concentration. Product formation (upper panel) did not exceed 4.3% of the total inosine. The lower panel shows examples of the determination of K_i* from a replot of v_s as a function of immucillin-H and immucillin-G concentration. The experimental points are values for v_s determined from fits of the data as shown in the upper panel.

$$\begin{array}{lll} \mathrm{I + E + A} \underset{k_2}{\overset{k_1}{\rightleftharpoons}} \mathrm{E{\cdot}A} \xrightarrow{k_{cat}} \mathrm{E + products} & & \\ k_3 \downarrow\uparrow k_4 & K_m = \dfrac{k_2 + k_{cat}}{k_1} & \\ \mathrm{E{\cdot}I} \underset{k_6}{\overset{k_5}{\rightleftharpoons}} \mathrm{E^*{\cdot}I} & K_i = k_4/k_3 & \\ & K_i^* = \dfrac{K_i k_6}{k_5 + k_6} & \end{array} \quad (2)$$

The enzyme (E) is assumed to be saturated with phosphate. The K_i value is the rapidly reversible dissociation constant for the PNP·immucillin complex (E·I). Slow onset of inhibition is determined by k_5, and the rate of relaxation from the transition-state PNP*·immucillin complex (E*·I) is k_6. Steps k_5 and k_6 are slower than all other steps. Values for K_i can be estimated from the effect of the inhibitors on the initial rate portion of the curve (Figure 2). Immucillin-H binds to the bovine enzyme with a K_i value of 41 ± 8 nM (Table 1). The K_i values for immucillin-H binding to human PNP and for immucillin-G binding to both human and bovine PNP enzymes are tighter and/or the value of k_5 is faster, since initial rate inhibition was not observed.

The slow-onset phase of the reaction, k_5, for bovine PNP with immucillin-H is 6.4×10^{-2} s^{-1} (Table 1). The relatively tight binding of the initial phase (K_i) made it necessary to use high concentrations of substrate to characterize the initial rate inhibition. Inosine binds with a K_m of 17 μM, and the use of 5 mM substrate permitted initial reaction rates to be observed for one minute or less (Figure 2). The slow-onset phase occurs in a well-defined transition characterized by a second steady-state rate (v_s) defined by the equilibrium shown in eq 2. In the presence of inhibitor and high substrate concentration, the steady-state inhibited phase occurs after a small fraction of substrate is converted to product. The expression also predicts that the onset of inhibition is dependent on both substrate and inhibitor concentration, since substrate and inhibitor compete for the catalytic site. The equilibrium inhibition constant, K_i*, is obtained from the v_s portion of the curve (Figure 2) and varies from 23 to 72 pM for human and bovine PNP with immucillin-H and immucillin-G (Table 1).

One-Third-the-Sites Inhibition. Following slow-onset inhibition, the release of bound inhibitor from the complex is also slow, permitting inhibitor titration of the enzyme. Titration of PNP with immucillin-H or immucillin-G, followed by incubation (3−4 h) to permit formation of the tightly bound complex, resulted in complete inhibition at one mole of immucillin per mole of enzyme trimer (Figure 3). The titration extrapolated to an inhibitory stoichiometry of 1.08 mol of inhibitor/mol of homotrimer. Similar results were obtained with immucillin-H and immucillin-G, and both inhibitors gave similar patterns with enzyme from human erythrocytes and from calf spleen. The subunit structure of mammalian PNP enzymes are homotrimeric with subunits of 32 000 M_r (*22*). The one-third-the-sites inhibition indicates that the subunits act in a sequential catalytic fashion with inhibitor at one of the three sites leading to complete inhibition. This proposal is supported by an earlier observation that in the absence of phosphate the calf spleen PNP homotrimer hydrolyzes inosine in a one-third-the-sites reaction to give the trimeric enzyme with one molecule of tightly bound hypoxanthine (K_d = 1.3 pM) and one mole of ribose released per trimer of enzyme (*12*). Crystallographic studies with PNP have indicated that the trimer contains three symmetrically disposed catalytic sites. Symmetric binding at all three catalytic sites occurs in crystal structures with substrate, product, and numerous inhibitors bound to the catalytic sites (*11*, *23*, *24*). In addition, equilibrium binding experiments with hypoxanthine establish one hypoxanthine binding site per monomer in the presence of phosphate (*12*).

All currently available results for PNP suggest that catalytic (transition-state) events occur at one site at a time, but reactant-state events (substrate, product, and ground-state analogue binding) can occur uniformly at all three sites. The inhibition of PNP by one mole of inhibitor per mole of trimer does not eliminate the possibility that the first molecule of immucillin bound inhibits the trimer, but additional molecules continue to bind tightly to the remaining two sites. Experiments to resolve these possibilities were accomplished by equilibrium ultrafiltration. Unbound inhibitor was determined by titration with known concentrations of PNP, using the relationship established in Figure 3. The results established that at the enzyme subunit-to-inhibitor ratio of 3:1 all inhibitor is bound to the enzyme. At subunit-to-inhibitor stoichiometries of 3:2 and 3:3, one and two equivalents of the inhibitors, respectively, are free (Table 2). The results establish that only one molecule of inhibitor is bound tightly

Table 1: Inhibition Constants for Transition-State Inhibitors of Purine Nucleoside Phosphorylase

	immucillin-H				immucillin-G			
enzyme	K_i[a] (nM)	k_5[b] ($s^{-1} \times 10^3$)	k_6[c] ($s^{-1} \times 10^5$)	K_i*[d] (pM)	K_i[a] (nM)	k_5[b] ($s^{-1} \times 10^3$)	k_6[c] ($s^{-1} \times 10^5$)	K_i*[d] (pM)
bovine PNP	41 ± 8	64 ± 40	4 ± 2	23 ± 5	*e*	*e*	19 ± 2	30 ± 6
human PNP	*e*	*e*	151 ± 65	72 ± 26	*e*	*e*	183 ± 70	29 ± 8

[a] K_i value was estimated by fitting initial rate data at various substrate and inhibitor concentrations to the equation for competitive inhibition using the Grafit program. [b] k_5 is estimated from K_i, K_i*, and k_6 using the relationship $k_5/k_6 = (K_i/K_i^*) - 1$. [c] k_6 is estimated from activity return experiments by fitting product concentration (P) versus time data to the equation $P = v_s t + (v_o - v_s)(1 - e^{-kt})/k$. The value of k derived from this experiment was an estimate of k_6 because the equation $k = k_6 + k_5(I/K_i)/[1 + (A/K_m) + (I/K_i)]$ reduces to $k = k_6$ under conditions where $I = 0$. [d] K_i* is estimated by fitting the data from a plot of v_s versus inhibitor concentration to the equation for standard competitive inhibition $v_s = (k_{cat}A)/[K_m(1 + (I/K_i^*) + A]$ and is expressed as the apparent dissociation constant for inhibitor from the trimer of PNP. [e] K_i is small and/or k_5 is fast, preventing the observation of steady-state inhibition under initial rate conditions.

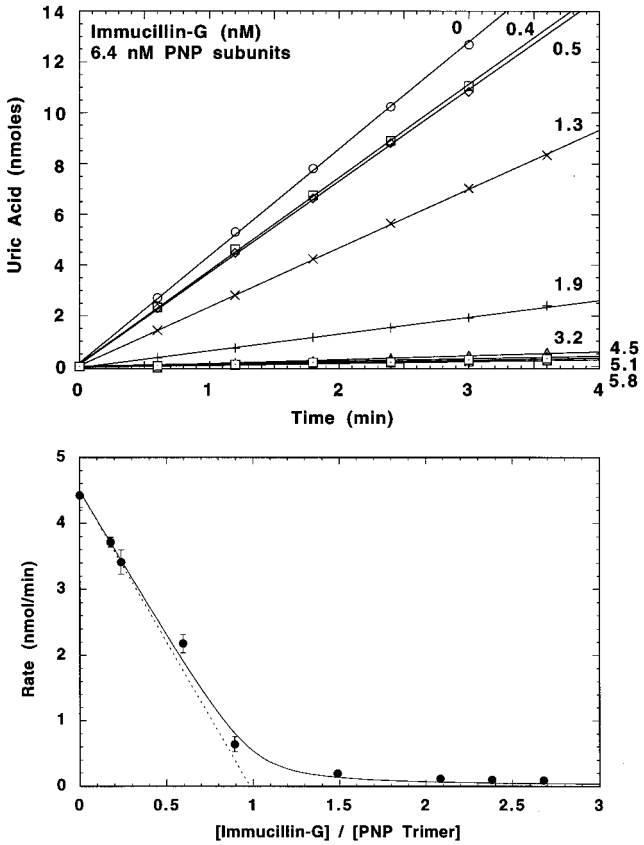

FIGURE 3: Immucillin-G titration of bovine spleen PNP (upper panel). Enzyme (6.4 nM subunits) and inhibitor at the indicated concentrations were incubated for 3 h at 30 °C under assay conditions but without inosine. The reactions were initiated by the addition of inosine to a final concentration of 40 μM, and the reaction was monitored by the UV change from the formation of uric acid in the coupled xanthine oxidase assay. In the lower panel, the initial rates of product formation are plotted as a function of moles of inhibitor per mole of PNP trimer. The line is fitted to the equation for interaction of tight-binding inhibitors (*18*).

Table 2: Binding Stoichiometry for Bovine PNP and Immucillins[a]

PNP subunits (μM)	3.0	3.0	3.0
immucillin-G (μM)	1.0	2.0	3.0
inhibitor bound to PNP (μM)	1.0 ± 0.1	1.2 ± 0.2	1.2 ± 0.2

[a] Equivalent results were obtained with immucillin-H.

to the PNP trimer, and it causes complete inhibition.

One-third-the-sites sequential catalysis in enzymes has been well characterized in the F_1 ATP synthase, which shares 3-fold structural and sequential site reaction properties with PNP (*13*). The intermediate reaction product, ATP, is tightly

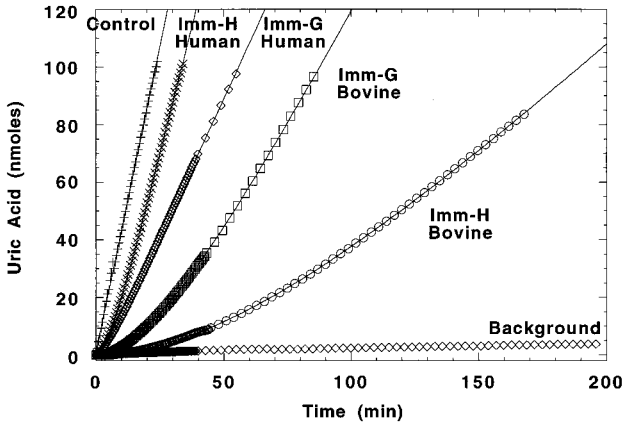

FIGURE 4: Dissociation of immucillins from bovine spleen and human PNP. Enzyme (64 μM subunits) and immucillins (64 μM) were incubated for 3 h at 30 °C followed by 40 000-fold dilution into an assay mixture containing 5 mM inosine, buffer, and xanthine oxidase. In the control experiments, an equivalent enzyme sample was treated in the same manner except that incubation was with buffer. The background shows the spectrophotometer response when no PNP is added to the otherwise complete reaction mixture.

bound to the enzyme in the same way that hypoxanthine is tightly bound to PNP following the hydrolytic reaction. Release of hypoxanthine in the catalytic cycle requires the presence of phosphate (*11*). It has been proposed that the transition-state binding energy for hypoxanthine is not released without formation and release of ribose 1-phosphate. The immucillins are transition-state inhibitors, which are proposed to capture the same energy because the inhibitors cannot be phosphorolyzed.

Slow Release of Bound Inhibitor. Transition-state inhibitors bind tightly but noncovalently at the catalytic site of PNP. Treatment of enzyme·immucillin-H complexes with heat (2 min at 95 °C), acid (3% trichloracetic acid), or base (50 mM KOH) caused release of inhibitor from the protein (data not shown). A time-dependent dissociation is expected for bound inhibitor following dilution of the enzyme·inhibitor complex into assay mixtures with no inhibitor. The tightly bound E*·I complex was formed by incubation of 68 μM enzyme subunits with 34 μM inhibitor to saturate one-third of the catalytic sites, leading to full inhibition and conditions where most of the inhibitor is bound to the enzyme. Rapid serial dilution of the E*·I complex into buffer (1:200) followed by dilution into the assay mixture (1:200) demonstrated time-dependent release of the inhibitor (Figure 4). At high concentrations of substrate the rate of activity regain can be used to estimate k_6, the first-order dissociation rate constant for the complex, which varied in the range $4-183 \times 10^{-5}$ s^{-1} for the complex (Table 1).

Biologically Effective Inhibition Constants. Half-times for dissociation of the binary complex ($t_{1/2} = 0.69/k_6$) vary from 6 min to 4.8 h for the inhibitors, with bovine PNP•-immucillin-H exhibiting the slowest off-rate (Table 1). Classical treatment using the subunit binding site concentration gives K_i^* values from 23 to 72 pM which is defined by the equilibrium binding constant $K_i^* = (E)(I)/(E^*•I)$.

Spectral Properties of the Inhibited Complex. The spectral properties of calf spleen PNP were determined by ultraviolet (UV), circular dichroism (CD), and fluorescence spectroscopy in the absence and presence of bound immucillin-H. Difference spectra were obtained by spectral subtraction in matched cuvettes or by electronic subtraction. The results show no changes greater than 5% of the spectral features, indicating that the environments of the three tryptophan residues and the relative content of α-helix and β-sheet experience only small changes as a consequence of transition-state inhibitor binding. Hinged domain motion which brings portions of the catalytic site together in the transition-state complex is consistent with these spectral changes. One-third-the-sites reactivity requires that binding of the inhibitor at one site alters the structure of the remaining two sites making them inaccessible to inhibitor. The same conformational occlusion occurs in the one-third-the-sites hydrolysis of inosine by PNP in the absence of inorganic phosphate (*12*). Proposals for dissociation of PNP trimer into active, monomeric, independent subunits have been reported (*25*), but these are not compatible with the stoichiometry of inhibitor binding reported here. Structural and mutational analyses of PNP have led to predictions for the changes in enzyme catalytic structure between substrate and transition-state binding (*11*, *22*, *26*), but these predictions are based on the interactions of ground-state inhibitors. The structural changes induced by the immucillin transition-state inhibitors reported here await the structural resolution of these complexes.

Structural Evidence for Number of Binding Sites. X-ray crystal structures of hypoxanthine, guanine, 9-deazainosine, and a variety of "structure-based inhibitors" bound to PNP demonstrate equivalent binding at all three of the catalytic sites of the trimer (*11*, *24*). Three equivalent hypoxanthine binding sites were also demonstrated for calf spleen PNP in the presence of phosphate and gave equivalent dissociation constants of 3 μM (*12*). Hypoxanthine saturation in the absence of phosphate caused formation of the complex with one hypoxanthine bound per trimer. This result has been explained by enzyme isomerization to the form with one tightly bound hypoxanthine (*12*). The one-third-the-sites tight binding of hypoxanthine in the hydrolytic reaction for inosine and for the immucillin transition-state inhibitors is proposed to be capturing transition-state binding energy. The one per subunit stoichiometry of substrate, product, and structure-based inhibitor interactions is proposed to be the stoichiometry for ground-state interactions for PNP. The transition-state inhibitors described here differ intrinsically from ground-state inhibitors. They bind 6 orders of magnitude more tightly than substrate and approximately 3 orders of magnitude more tightly than previously reported inhibitors. One-third-the-sites inhibitory activity is only associated with transition-state interactions.

Molecular Electrostatic Potential Surfaces of Transition State and Inhibitor. Enzymes are proposed to bind tightly to their cognate transition-states because of the altered electron distribution at the van der Waals surface relative to that of the substrate (*27*−*29*). Matching the electrostatic features of the transition-state in a stable transition-state inhibitor is therefore expected to lead to transition-state inhibitors. Examples of this phenomenon have been documented for nucleoside hydrolase, AMP deaminase, and AMP nucleosidase (*20*, *28*, *30*, *31*). The molecular electrostatic potential surfaces for substrate, transition-state, and immucillin-H were compared. The substrate is a neutral molecule, while the transition-state carries a net positive charge, which is delocalized through the ribosyl and purine rings. The inhibitor can be protonated at the nitrogen of the iminoribitol ring ($pK_a = 6.5$); however the protonation state of bound immucillins is unknown. Unprotonated 1-substituted iminoribitols are proposed to bind to the related nucleoside hydrolases (*28*, *32*). For similarity comparisons, the substrate and inhibitor are compared to the transition-state. The ab initio calculations of the electrostatic potential surfaces were therefore performed for the neutral substrate and neutral inhibitor but with charged transition-state. The similarity comparison calculations were performed with the average electrostatic potential over all surface points for each molecule scaled to be 0. The relative distribution of positive regions on the molecular surfaces dictates the enzymatic recognition process, rather than the magnitude of the absolute charge. The similarity comparison results indicate that the similarity of substrate to the transition-state is 0.483 while the similarity of immucillin-H to the transition-state is 0.723 (Figure 5). The similarity of the transition-state to itself is 1.00. The inhibitor is electrostatically and geometrically more similar to the transition-state than is the substrate inosine, and the inhibitor binds more tightly. A plot of the free energy of binding for substrate, substrate analogues, transition-state analogues, and transition-state as a function of $<S_e>$ gives a near-linear correlation for several enzymes (*20*). For PNP, the dimensionless binding free energy $\Delta G/RT$ of inosine, inhibitor, and transition-state when plotted against the similarity of each species to the transition-state also gives a straight line relationship (Figure 5). As calculated from this algorithm, a similarity value of 0.723

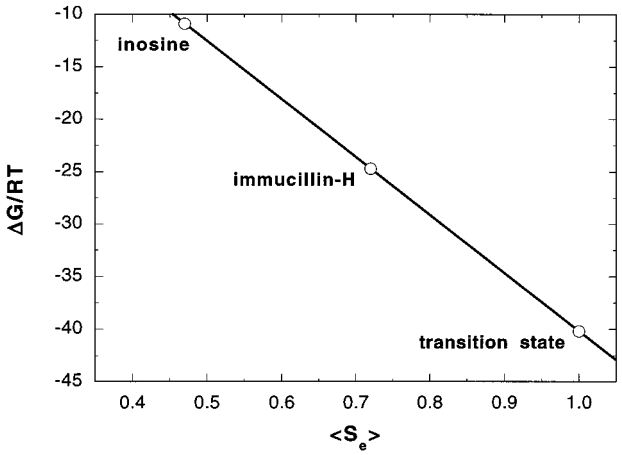

FIGURE 5: Relationship between the dimensionless binding free energy ($\Delta G/RT$) and the molecular electrostatic potential surface similarity $\langle S_e \rangle$ for inosine, immucillin-H, and the transition-state. The straight line connects the experimental value of $\Delta G/RT$ for the substrate and the calculated $\Delta G/RT$ for the transition-state (Figure 1). The coordinates for the immucillin-H point were determined experimentally and computationally as described in the text.

for the inhibitor predicts a $\Delta G/RT$ for binding of −25.5 compared to that of −24.9 observed experimentally. By contrast, a $\Delta G/RT$ of −10.8 is observed for inosine, and the estimated $\Delta G/RT$ for binding the transition-state is −40.3. Even though the immucillin inhibitors are the most powerful yet reported for the enzyme, they remain 9 kcal/mol (or 15.4 in $\Delta G/RT$ units) from transition-state binding perfection. Perfect transition-state inhibitors are rare due to the non-equilibrium bond lengths which define the substrate at the transition state and to the strong dependence of hydrogen bond energy on small changes in H-bond lengths and angles (*33*). Fortunately, only a small fraction of the large energy of transition-state binding is required to provide inhibitors which are powerful enough for physiological efficiency. The inhibitory affinity of the immucillins is exemplified by the observation that less than 0.002 mg of the inhibitors is needed to convert the water volume of a human (approximately 30 L) to a concentration of 200 pM, well above the K_i* values established for these inhibitors with mammalian PNP.

Conclusions. The transition-state inhibitors immucillin-H and immucillin-G bind to mammalian PNP with equilibrium dissociation constants from 23 to 72 pM. Binding is slow-onset, tight binding, and dissociation of the enzyme·inhibitor complex is slow, for example bovine PNP·immucillin-H has a $t_{1/2}$ for dissociation of 4.8 h. The inhibitor binds to a single subunit of the PNP homotrimer to give complete inhibition, establishing one-third-the-sites interactions for transition-state events with this enzyme.

ACKNOWLEDGMENT

The authors thank Paul J. Berti for his help in figure preparation.

REFERENCES

1. Hershfield, M. S., and Mitchell, B. S. (1995) in *The Metabolic Basis of Inherited Disease* Scriber, C. R., Beaudet, A. L., Sly, W. S., Valle, D., Eds. 7th ed., Chapter 52, pp 1725−1768, McGraw-Hill, Inc., New York.
2. Janeway, C. A., Jr., and Travers, P. (1997) *Immunobiology*: *The Immune System in Health and Disease*, 3rd ed., Current Biology Ltd./Garland Publishing Co., London and New York.
3. Bantia, S., Montgomery, J. A., Johnson, H. G., and Walsh, G. M. (1996) *Immunopharmacology 35*, 53−63.
4. Thelander, L., and Reichard, P. (1979) *Annu. Rev. Biochem. 48*, 133−158.
5. Snyder, F. F., Jenuth, J. P., Mably, E. R., and Mangat, R. K. (1997) *Proc. Natl. Acad. Sci. U.S.A. 94*, 2522−2527.
6. Boehncke, W.-H., Gilbertsen, R. B., Hemmer, J., and Sterry, W. (1994) *Scand. J. Immunol. 39*, 327−332.
7. Montgomery, J. A., Niswas, S., Rose, J. D., Secrist, J. A., III, Babu, Y. S., Bugg, C. E., Erion, M. D., Guida, W. C., and Ealick, S. E. (1993) *J. Med. Chem. 36*, 55−69.
8. Niwas, S., Chand, P., Pathak, V. P., and Montgomery, J. A. (1994) *J. Med. Chem. 37*, 2477−2480.
9. Walsh, G. M., Reddy, N. S., Bantia, S., Babu, Y. S., and Montgomery, J. A. (1994) *Hematol. Rev. 8*, 87−97.
10. Kline, P. C., and Schramm, V. L. (1993) *Biochemistry 32*, 13212−13219.
11. Erion, M. D., Stoeckler, J. D., Guida, W. C., Walter, R. L., and Ealick, S. E. (1997) *Biochemistry 36*, 11735−11748.
12. Kline, P. C., and Schramm, V. L. (1992) *Biochemistry 31*, 5964−5973.
13. Boyer, P. D. (1997) *Annu. Rev. Biochem. 66*, 717−749.
14. Stoeckler, J. D., Agarwal, R. P., Agarwal, K. C., and Parks, R. E., Jr. (1978) *Methods Enzymol. 51*, 530−538.
15. Kim, B. K., Cha, S., and Parks, R. E., Jr. (1968) *J. Biol. Chem. 243*, 1763−1770.
16. Furneaux, R. H., Limberg, G., Tyler, P. C., and Schramm, V. L. (1997) *Tetrahedron 53*, 2915−2930.
17. Lim, M.-I., Ren, W.-Y., Otter, B. A., and Klein, R. S. (1983) *J. Org. Chem. 48*, 780−788.
18. Morrison, J. F., and Walsh, C. T. (1988) *Adv. Enzymol. Relat. Areas Mol. Biol. 61*, 201−301.
19. Bagdassarian, C. K., Braunheim, B. B., Schramm, V. L., and Schwartz, S. D. (1996) *Int. J. Quantum Chem. 23*, 73−80.
20. Bagdassarian, C. K., Schramm, V. L., and Schwartz, S. D. (1996) *J. Am. Chem. Soc. 118*, 8825−8836.
21. Frisch, M. J., Trucks, G. W., Hend-Gordon, M., Gill, P. M. W., Wong, M. W., Foresman, J. B., Johnson, B. G., Schlegel, H. B., Robb, M. A., Replogle, E. S., Gomperts, R., Andres, J. L., Raghavachari, K., Binkley, J. S., Gonzalez, C., Martin, R. L., Fox, D. J., DeFrees, D. J., Baker, J., Stewart, J. J. P., and Pople, J. A. (1992) *Gaussian 92 user's guide*, Gaussian Inc., Pittsburgh, PA.
22. Ealick, S. E., Rule, S. A., Carter, D. C., Greenhough, T. J., Babu, Y. S., Cook, W. J., Habash, J., Helliwell, J. R., Stoeckler, J. D., Parks, R. E., Jr., Chen, S. F., and Bugg, C. E. (1990) *J. Biol. Chem. 265*, 1812−1820.
23. Erion, M. D., Takabayashi, K., Smith, H. B., Kessi, J., Wagner, S., Honger, S., Shames, S. L., and Ealick, S. E. (1997) *Biochemistry 36*, 11725−11734.
24. Koellner, G., Luić, M., Shugar, D., Saenger, W., and Bzowska, A. (1997) *J. Mol. Biol. 265*, 202−216.
25. Ropp, P. A., and Traut, T. W. (1991) *J. Biol. Chem. 266*, 7682−7687.
26. Stoeckler, J. D., Poirot, A. F., Smith, R. M., Parks, R. E., Jr., Ealick, S. E., Takabayashi, K., and Erion, M. D. (1997) *Biochemistry 36*, 11749−11756.
27. Horenstein, B. A., and Schramm, V. L. (1993) *Biochemistry 32*, 7089−7097.
28. Horenstein, B. A., and Schramm, V. L. (1993) *Biochemistry 32*, 9917−9925.
29. Schramm, V. L., Horenstein, B. A., and Kline, P. C. (1994) *J. Biol. Chem. 269*, 18259−18262.
30. Deng, H., Chan, A. W.-Y., Bagdassarian, C. K., Estupiñán, B., Ganem, B., Callender, R. H., and Schramm, V. L. (1996) *Biochemistry 35*, 6037−6047.
31. Ehrlich, J. I., and Schramm, V. L. (1994) *Biochemistry 33*, 8890−8896.
32. Parkin, D. W., and Schramm, V. L. (1995) *Biochemistry 34*, 13961−13966.
33. Smallwood, C. J., and McAllister, M. A. (1997) *J. Am. Chem. Soc. 119*, 11277−11281.

BI980658D